Supporting Information

Poly(*N*-cyanoethylacrylamide), a new thermoresponsive homopolymer presenting both LCST and UCST behavior in water

Nicolas Audureau, Fanny Coumes, Jutta Rieger*, François Stoffelbach*

Sorbonne Université, CNRS, UMR 8232, Institut Parisien de Chimie Moléculaire (IPCM), Polymer Chemistry Team, 4 Place Jussieu, 75252 Paris Cedex 05, France

E-mail: jutta.rieger@sorbonne-universite.fr; francois.stoffelbach@sorbonne-universite.fr

Content

1. Additional Protocols

1.1. Determination of *dn/dC* by size exclusion chromatography measurements

The refractive index increment (*dn*/*dC*) was measured with the online RI detector by injecting polymer (**P3, Table 1**) solutions at different concentrations (**Figure S1**). The *dn/dC* was calculated by plotting the RI area (integrated from the RI signal) versus the injected concentration with the OmniSEC software from the slope of the straight-line using **Equation 1**:

$$RI_{area} = \frac{K_{RI}}{n_0} \times \frac{dn}{dC} \times V_{inj} \times [C] \qquad \textbf{(Equation 1)}$$

with n_0, the refractive index of the solvent, V_{inj}, the injection volume of the polymer solution (mL), K_{RI}, the refractometer constant (mV) and [C], the polymer solution concentration (g mL^{-1}).

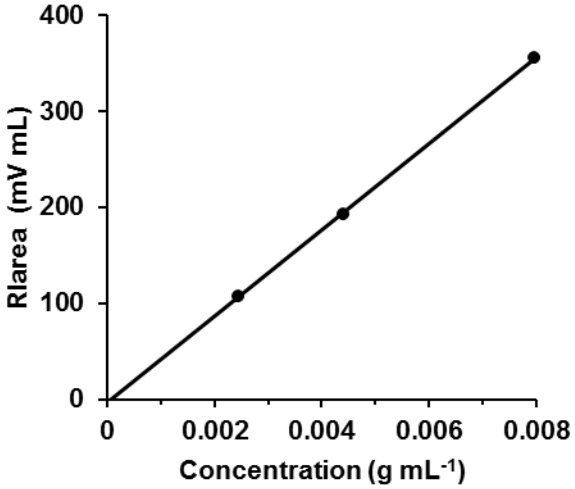

Figure S1. Plot of RI_{area} versus the polymer concentration for the determination the *dn/dC*.

1.2. Determination of molar composition of P(CEAm-*co*-CMAm) using the individual monomer conversions (determined by ^{1}H NMR in DMSO-d_6)

During and at the end of the copolymerizations, aliquots were taken and analyzed by ^{1}H NMR in DMSO-d_6 to determine the individual molar conversions of CEAm and CMAm by the relative integration of the signals characteristic of one vinylic proton of the comonomers (for CMAm at 5.70 ppm and for CEAm at 5.61 ppm) and of a reference signal at ~7.9 ppm (corresponding to the DMF proton, **H-**CO).

1.3. Determination of molar composition of P(CEAm-*co*-CMAm) purified by precipitation by ^{1}H NMR in DMSO-d_6

The copolymers were analyzed by ^{1}H NMR to determine the molar fraction of CMAm in the copolymer by the integration of the signal at ~4.1 ppm corresponding to the C**H**$_2$-CN protons of the CMAm monomer units and the integration of the signal between 1 and 2.3 ppm corresponding to the protons of the backbone C**H**$_2$-C**H** from the CEAm and CMAm monomer units.

An example is shown in **Figure S11** for P(CEAm$_{0.90}$-*co*-CMAm$_{0.10}$)$_{192}$ (**P8**, **Table 2**).

1.4. Determination of molar composition of P(CEAm-co-Am) using the individual monomer conversions (determined by ^{1}H NMR in DMSO-d_6)

During and at the end of the copolymerizations, aliquots were taken and analyzed by ^{1}H NMR in DMSO-d_6 to determine the individual molar conversions of Am and CEAm by the relative integration, of the integration at 5.56 ppm corresponding to a part of the vinylic protons (**H**$_2$C=CH) of the residual Am and the integration of the vinylic protons (**H**$_2$C=C**H**) of both

residual comonomers between 5.54 and 5.68 ppm and of a reference signal at ~2.9 ppm (corresponding to one of the methyl groups of DMF).

1.5. Determination of molar composition of P(CEAm-*co*-Am) purified by precipitation by ^{1}H NMR in DMSO-d_6

The copolymers were analyzed by ^{1}H NMR to determine the molar fraction of Am in the copolymer by the integration of the signal at ~2.7 ppm corresponding to the C**H**$_2$-CN protons of the CEAm monomer units and the integration of the signal between 1 and 2.3 ppm corresponding to the protons of the backbone C**H**$_2$-C**H** from the CEAm and Am units.

An example is shown in **Figure S12** for P(CEAm$_{0.98}$-*co*-Am$_{0.02}$)$_{195}$ (**P11**, **Table S2**).

2. Additional data

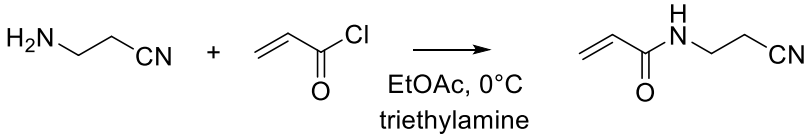

Scheme S1. Synthesis route of *N*-cyanoethylacrylamide.

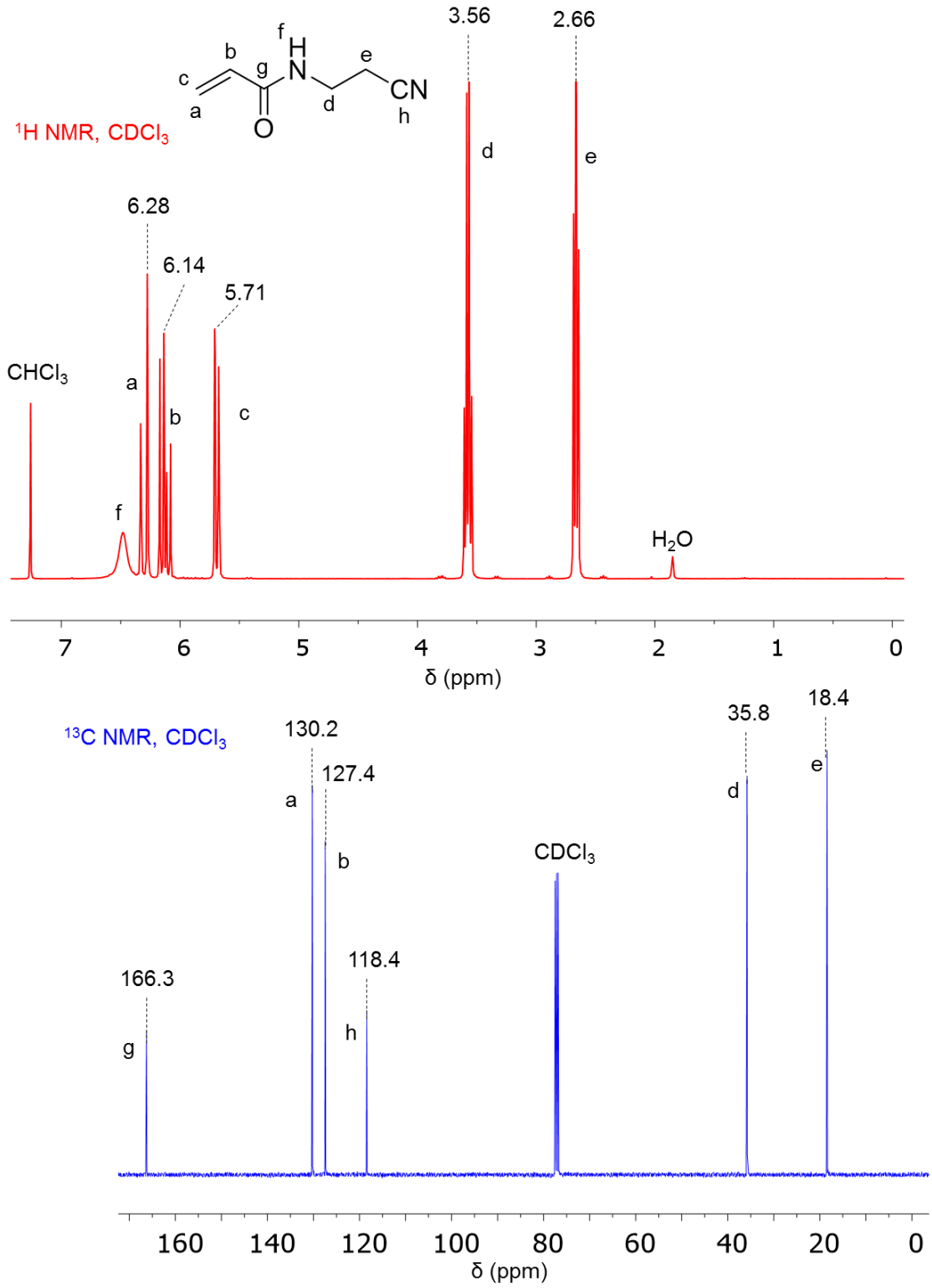

Figure S2. ^{1}H and ^{13}C NMR spectra of CEAm recorded in $CDCl_3$.

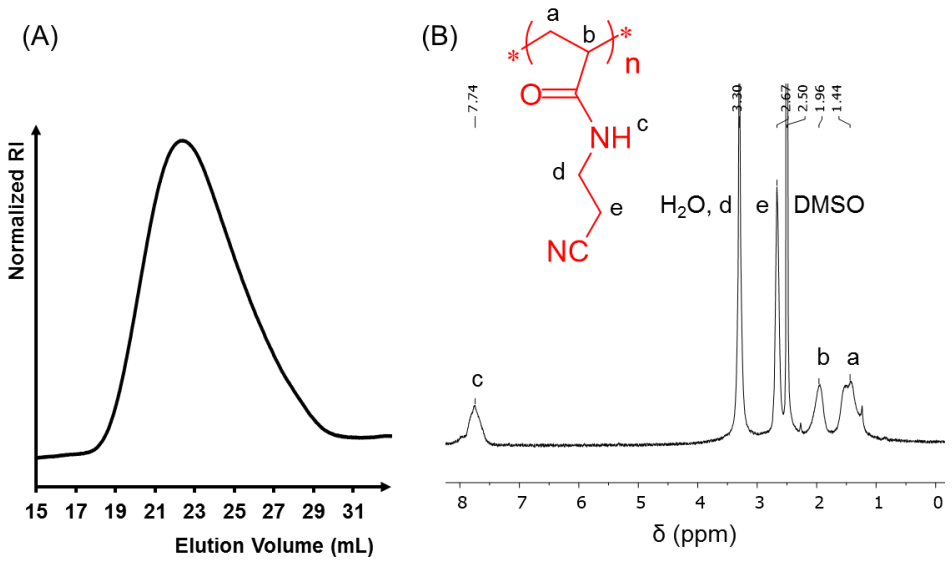

Figure S3. (A) Normalized SEC chromatogram in DMF (+LiBr 1g L^{-1}) and (B) ^{1}H NMR spectrum in DMSO-d_6 of PCEAm obtained by FRP after purification by precipitation in chloroform (**P7**, **Table 1**).

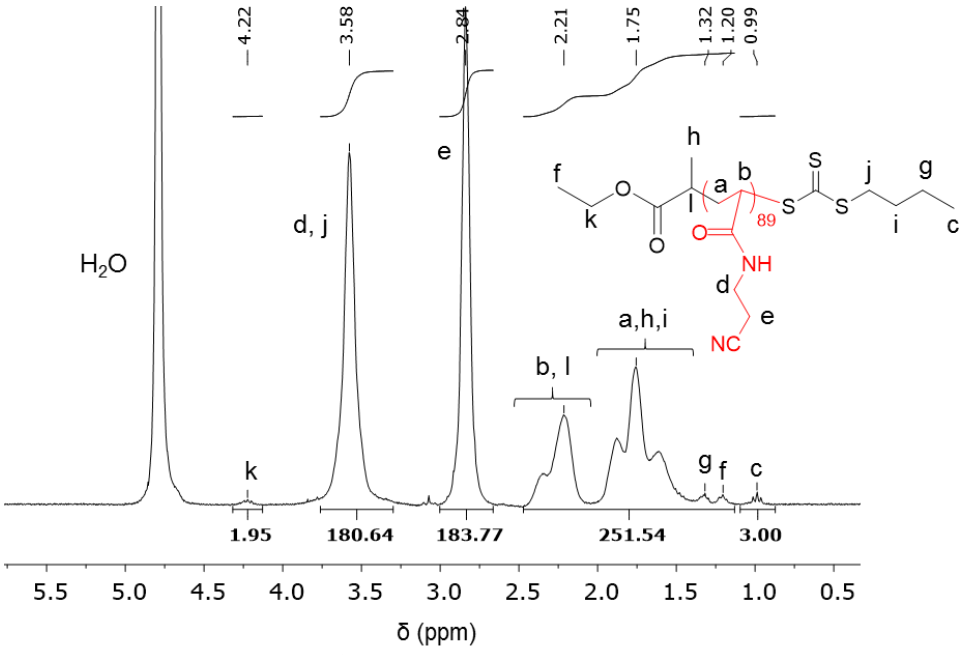

Figure S4. ^{1}H NMR spectrum in D_2O of $PCEAm_{89}$ obtained by RAFT polymerization (**P1**, **Table 1**).

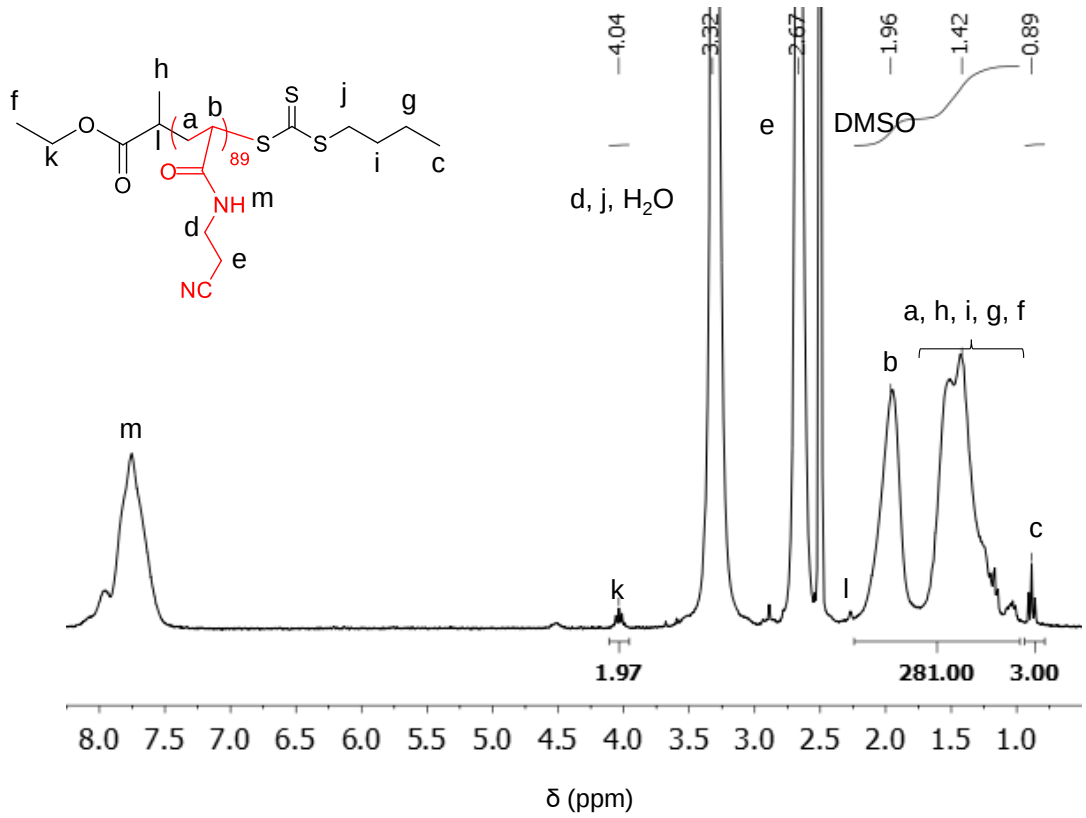

Figure S5. ^{1}H NMR spectrum in DMSO-d_6 of $PCEAm_{89}$ obtained by RAFT polymerization (**P1**, **Table 1**).

Note: ^{1}H NMR in D_2O (**Figure S4**) and DMSO-d_6 (**Figure S5**) confirmed the presence of the CTA-1 in the polymer chains with the C**H**$_3$ end-chain of CTA-1 visible at δ = 0.9-1.0 ppm. Using this signal as reference and comparing the proton integrations of either the backbone or the side-chain (**Figure S4**), the number-average degree of polymerization ($DP_{n,exp}$) could be calculated to be 80 and 90 respectively, which is close to the theoretical value ($DP_{n,th}$ = 89). The significantly lower value calculated using the protons of the PCEAm backbone might be attributed to a partial aggregation of the polymer chains during the ^{1}H NMR analysis performed at 27 °C. The polymer solution was actually slightly turbid in D_2O, and we can therefore assume that the protons from the backbone are less mobile than the protons belonging to the side-chains, which might explain their reduced integration. Analysis of the polymer in DMSO-d_6 (**Figure S5**), in which the polymer is fully soluble, gave a DP_n very close to the expected value using the backbone protons. In summary, the combined SEC and ^{1}H-NMR results confirmed a chain end-functionalization by the CTA-1 close to 100%. It should be noted that for higher targeted DP_n, the CH_3 end-chain became less visible in the ^{1}H NMR spectra making accurate $DP_{n,exp}$ determination impossible. As the theoretical DP_n determined by the monomer conversion, $DP_{n,th}$, were in good agreement with the experimental values, $DP_{n,exp}$, the $DP_{n,th}$ was used for further calculations.

Table S1. Experimental results for the polymer **P4bis** (replica of P4 in Table 1)

Entry	$DP_{n,th}$[a]	$M_{n,th}$[a] (kg mol^{-1})	$M_{n,SEC}$[b] (kg mol^{-1})	$Đ$[b]	T_{CP}[c] (°C)	
					LCST	UCST
P4bis	211	26.4	36.7	1.23	39/41	77/77

[a] Theoretical number-average degree of polymerization, $DP_{n,th}$, and theoretical number-average molar mass, $M_{n,th}$, calculated using the experimental conversion. [b] Number-average molar mass, M_n, and dispersity, $Đ$, determined by SEC in DMF (+ LiBr 1g L^{-1}) with a PMMA calibration. [c] Determined in water by turbidimetry at 1 wt%, on 1st cooling/2nd heating.

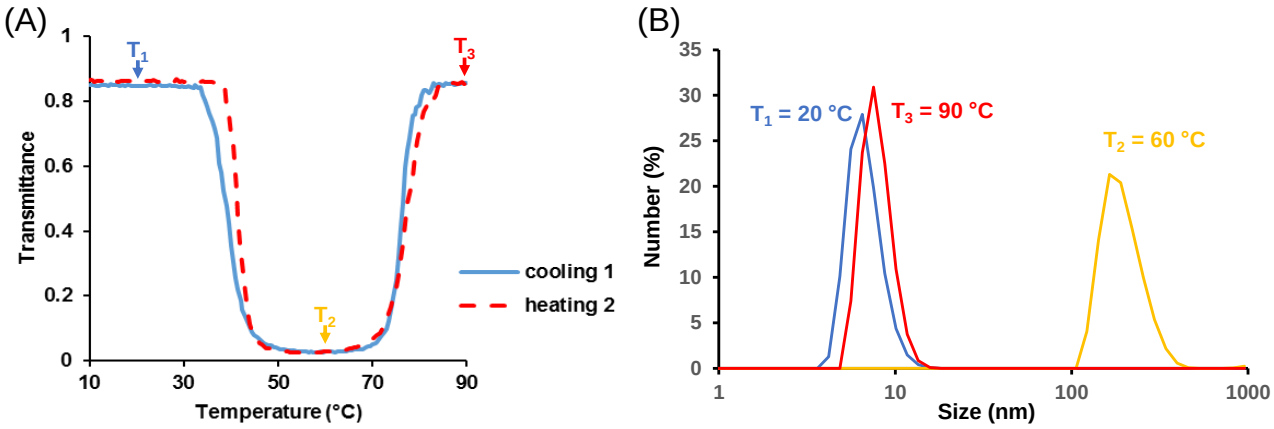

Figure S6. (A) Turbidity curves (first cooling and second heating) of **P4bis** at 1 wt% in water (**Table S1**). (B) Overlay of DLS profiles of **P4bis** at 1 wt% in water at 20, 60 and 90 °C.

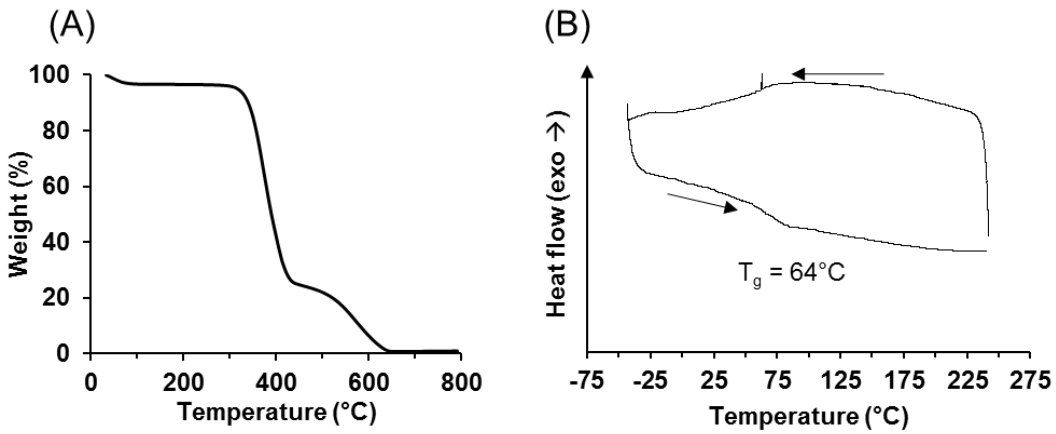

Figure S7. (A) TGA analysis under air and (B) DSC analysis of poly(*N*-cyanoethylacrylamide) (PCEAm) prepared by free radical polymerization (**P7**, **Table 1**).

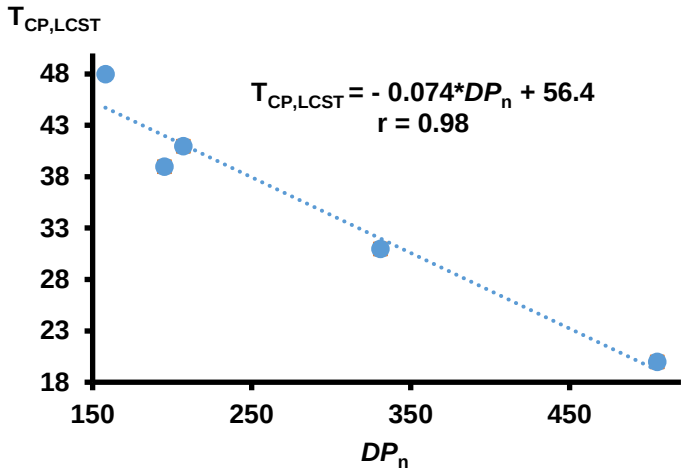

Figure S8. Evolution of $T_{CP,LCST}$ (cooling step) versus the DP_n of the homopolymers of PCEAm (P2-P6 in Table 1).

(A)

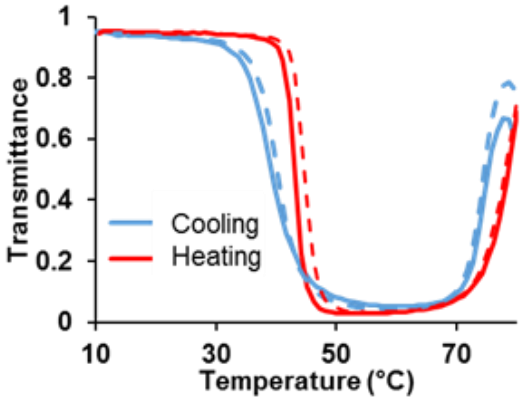

(B)

Cycle	$T_{CP,LCST}$ (°C) cooling/heating	$T_{CP,UCST}$ (°C) cooling/heating
1	39/43	75/79
2	41/45	75/78

Figure S9. (A) Turbidity curves of two consecutive cycles of $PCEAm_{195}$ (**P3**, **Table 1**) at 1 wt% in water, solid lines for the first cycle and dashed line for second one. (B) LCST and UCST T_{CP} for each cycle during heating and cooling step.

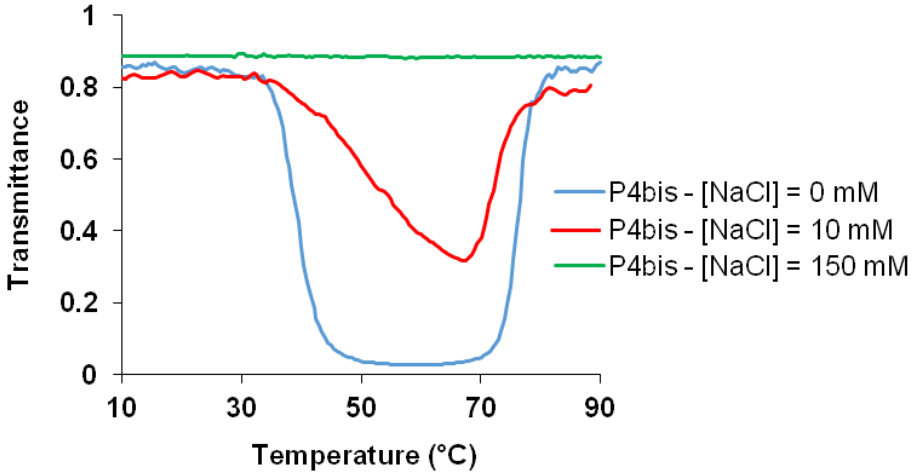

Figure S10. Influence of sodium chloride addition ([NaCl] from 0 to 150 mM) on temperature dependence of optical transmittance (cooling step) for $PCEAm_{211}$ (**P4bis**, **Table S1**) aqueous solution (1 wt%).

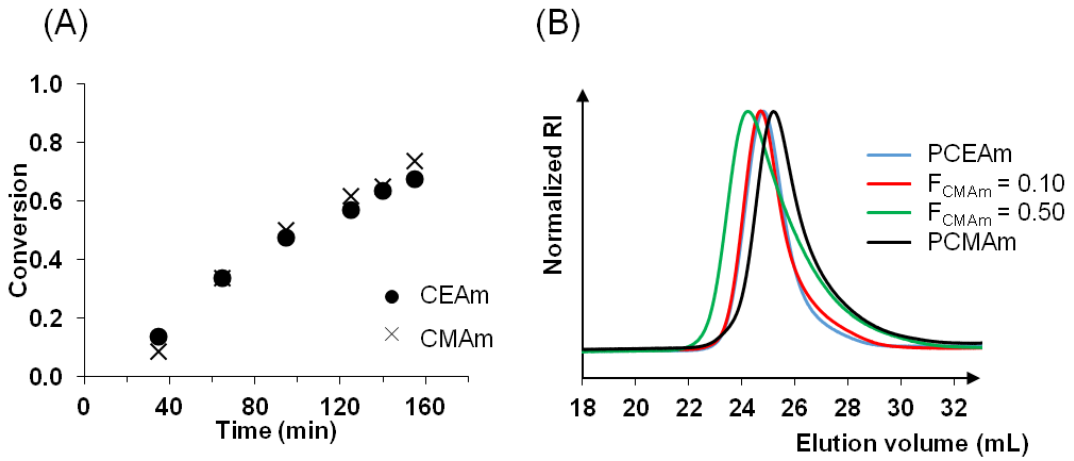

Figure S11. (A) Monomer conversions monitored by ^{1}H NMR in DMSO-d$_6$, (**P8**, **Table 2**) and (B) SEC chromatograms in DMF (+LiBr 1g L^{-1}) of P(CEAm-*co*-CMAm) (red and green curves) and the corresponding PCEAm (blue) and PCMAm (black) homopolymers (**P3**, **P8-10**, **Table 2**).

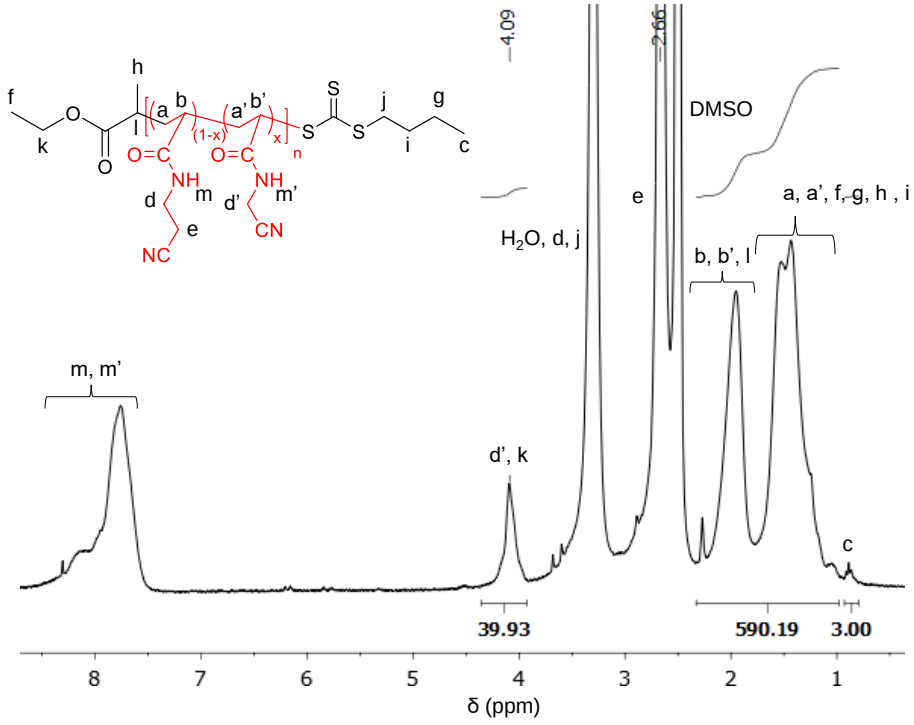

Figure S12. ^{1}H NMR spectrum in DMSO-d$_6$ of P(CEAm-*co*-CMAm) (**P8**, **Table 2**) obtained by RAFT polymerization.

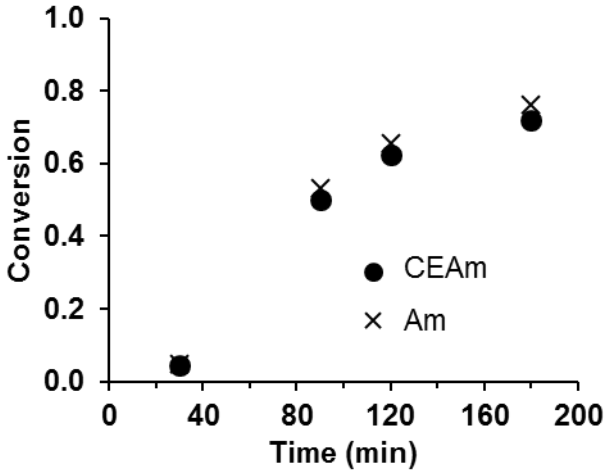

Figure S13. Monomer conversions monitored by ^{1}H NMR in DMSO-d_6 (**P12**, **Table S2**).

Table S2. Experimental conditions for the synthesis of P(CEAm-*co*-Am) copolymers in the presence of CTA-1and their characteristics[#]

Entry	mol% of Am[a]	$[M]_0$/ $[CTA\text{-}1]_0$	Time (h)	Conv.[b] (mol%)		mol% of Am[c]	F_{Am}[d]	$DP_{n,th}$[e]	$M_{n,th}$[e] (kg mol^{-1})	$M_{n,SEC}$[f] (kg mol^{-1})	$Đ$[f]	T_{CP} (at 4 wt% in water)[g] (°C)	
				CEAm	Am							LCST	UCST
P4bis	0	270/1	3.3	78	-	0	0	211	26.4	36.7	1.23	44	77
P11	2.0	260/1	2.2	75	76	2.4	0.02	195	24.3	34.0	1.20	41	74
P12	8.4	270/1	3.0	72	76	10	0.09	196	26.3	30.2	1.28	soluble	

[#]Polymerizations were performed in DMF at 70 °C in presence of the RAFT agent CTA-1 and AIBN as a radical initiator at 20 wt% at an initial molar ratio of CTA-1/AIBN: 1/0.1. [a] Initial mol% of Am in the mixture of monomers. [b] Individual monomer conversions determined by ^{1}H NMR analysis. [c] mol% of Am in the copolymer deduced from the experimental conversions. [d] Molar fraction of Am in the purified copolymer deduced from ^{1}H NMR analysis. [e] Theoretical number-average degree of polymerization, $DP_{n,th}$, and theoretical number-average molar mass, $M_{n,th}$, calculated using the experimental conversions. [f] Number-average molar mass M_n and dispersity, $Đ$, determined by SEC in DMF (+ LiBr 1g L^{-1}) with a PMMA calibration. [g] Determined by turbidimetry during the heating step.

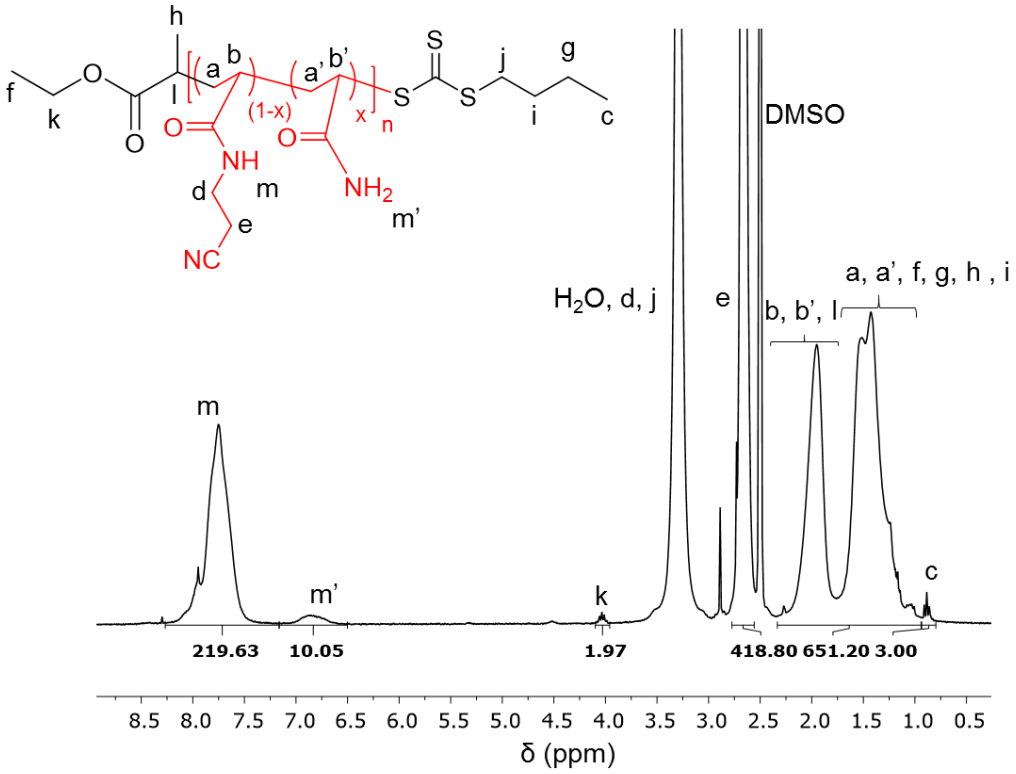

Figure S14. ^{1}H NMR spectrum in DMSO-d_6 of P(CEAm-*co*-Am) (**P11**, **Table S2**) obtained by RAFT polymerization.

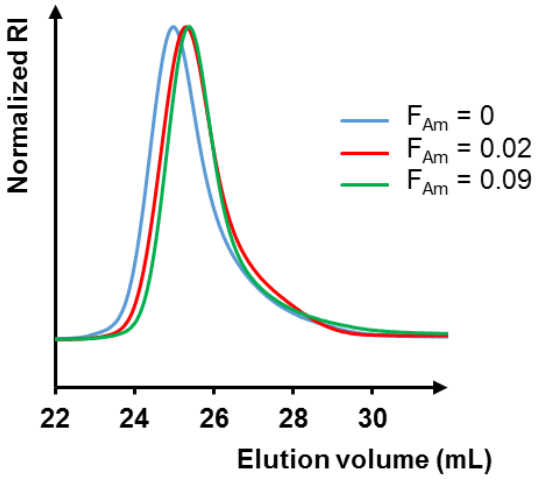

Figure S15. SEC chromatograms in DMF (+ LiBr) for the RAFT copolymerizations of CEAm with Am by targeting different F_{Am} (**P4bis**, **P11-12**, **Table S2**).

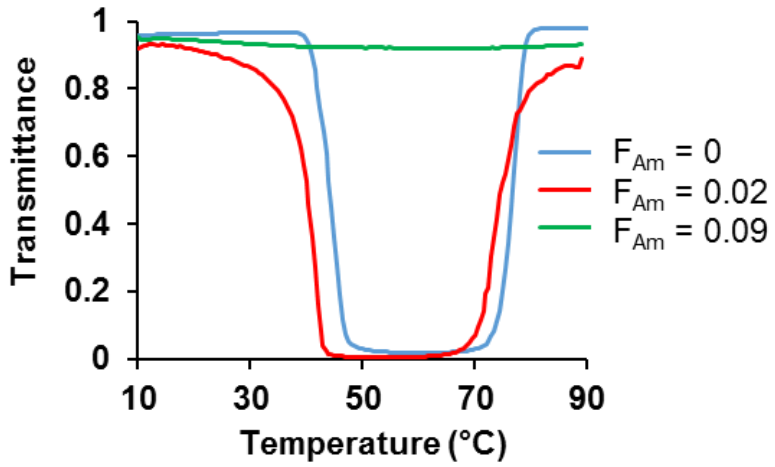

Figure S16. Influence of F_{Am} on temperature dependence of optical transmittance for copolymers of CEAm with Am with different F_{Am} (**P4bis**, **P11-12**, **Table S2**) in aqueous solution (4 wt%) (heating step).

Figure S17. Photos of **P11** (**Table S2**) at 4 wt% in water at different temperatures.